Diffusion-controlled kinetics of protein domain coalescence: Effects of orientation, interdomain forces and hydration[a)]

Gary P. Zientara

Engineering-Science, McLean, Virginia 22102

Janice A. Nagy[b)] and Jack H. Freed

Department of Chemistry, Cornell University, Ithaca, New York 14853
(Received 22 May 1980; accepted 1 August 1980)

The numerical methods of Zientara and Freed [J. Phys. Chem. **83**, 3333 (1979)] have been used to study the diffusion-controlled kinetics of domain coalescence in order to ultimately consider the time evolution of protein folding. The mean coalescence lifetime for a domain pair has been calculated using the eigenfunction expansion method and finite differences in the solution of a modified form of the Smoluchowski equation. This approach allows for an orientational preference in the domain coalescence process, which has been studied throughout the complete range of reactivities. Three cases of interdomain forces were investigated, one of which represents the shielding of charged domains by ions in solution. As the forces vary from the strongly repulsive to the strongly attractive in these cases, the coalescence lifetime decreases by several orders of magnitude. In addition, a hydration shell model, which provides an activation barrier to coalescence, has been analyzed. The lifetimes resulting from this model were observed to depend strongly on the location and extent of the hydration shell. Anisotropic initial conditions were also incorporated causing, in some cases, non-negligible effects upon the coalescence lifetimes.

I. INTRODUCTION

Karplus and Weaver[1] have recently suggested a model of protein microdomain coalescence based on a diffusion-controlled kinetic treatment of the microdomain motion in a liquid solvent to explain the dynamics of the protein folding process. Protein folding processes have generated a considerable number of studies in the past.[2] The term "protein folding" is used to denote the process of conversion of a randomly coiled polypeptide chain into the unique three-dimensional conformation of the native protein.[2] In the "diffusion-collision" model of Karplus and Weaver, the protein molecule is divided into several independent microdomains that must diffuse together and collide in order to coalesce into a structural entity with the native conformation. The entire folding process would then involve a series of such diffusion-collision steps.

The concept of nucleation in one or several limited regions of the polypeptide chain has been suggested by many authors.[3] Nucleation is thought to involve portions of the chain that are near each other in sequence. A subsequent growth and/or coalescence of these regions into larger units during later stages of the folding process leads ultimately to the folded protein.[3] Theoretical arguments propose that not all of conformational space is sampled in a statistical mechanical sense by the molecule during the folding of the polypeptide chain, as this would require too much time.[4] (Fully random sampling for a protein of 150 amino acids would require 10^{26} years or more,[2] while proteins folding *in vivo* during synthesis or *in vitro* during renaturation require folding times on the order of seconds or minutes.)[5] Experimental evidence[6] supports the theory that protein folding is not a random process and suggests that certain intermediate conformations are favored during protein folding. The existence of distinct structural domains within the folded states of many large proteins,[7] as determined by x-ray crystallography, also lends credence to the concept of a directed pathway of folding.

Karplus and Weaver have applied arguments of diffusion-controlled kinetics to derive the basic equations for the time dependence of the coalescence of two diffusing spherically symmetric microdomains. They emphasize this as an elementary step in the diffusion-collision-coalescence model of protein folding. The diffusive character of the microdomains (referred to hereafter as "domains") emerged from an analysis of molecular dynamics protein studies[8-10] and is related to similar diffusional studies of polymer chain segments.[11] Clearly, the aggregation of segments of the polypeptide chain that have already undergone a transition from random-coil to native or near-native structures can be described by diffusion-controlled kinetics[12] if the domains move independently in the solvent.

Incorporating the effects of a connecting chain with a finite size, charged domains, domains with preferred coalescence sites, and an anisotropic initial domain pair distribution leads to complications beyond the scope of the solutions available from analytical mathematical treatments. Theoretical and computational exploration of time-dependent protein and polymer chain processes employing either molecular dynamics[8,9,13] or stochastic dynamics methods[14] reveal correlations of chain segments and short time scale (i.e., nanosecond) behavior. It is not computationally feasible, however, to use these methods to generate the entire time evolution of a protein's native tertiary structure from an initially unfolded state.

[a)]Supported by NSF Grant No. CHE-77-26996 and by NIH Grant No. GM25862-02.
[b)]NIH Predoctoral Fellow, 1977–1980.

 0021-9606/80/225092-15$01.00

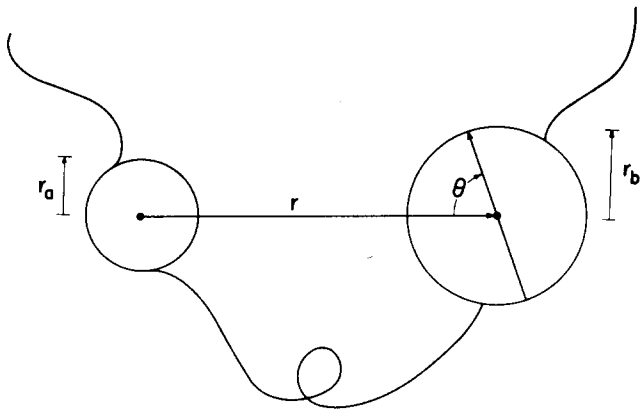

FIG. 1. Schematic diagram of two spherical domains situated along a flexible chain with one domain exhibiting an angular dependence in its reactivity about a preferred axis.

In this work we include in a diffusion-controlled kinetic analysis of domain coalescence the orientation dependence of the protein domains' reactivity and allow for complex interactions between these domains. The solution of the resulting problem is accomplished by the use of the numerical methods of Zientara and Freed,[15] modified to obtain the mean lifetimes of an uncoalesced pair of domains (i.e., the mean coalescence time). This approach uses both the eigenfunction expansion method and finite differences in the solution of a modified form of the Smoluchowski equation.[16] This allows us to easily treat anisotropic domain properties in an orientation dependent diffusion-controlled reaction scheme by including both translational and rotational diffusion.[17-21]

The theoretical details of this treatment appear in Sec. II. A discussion of the numerical methods used may be found in Sec. III. The effects of several types of domain–domain interactions on the mean coalescence time are analyzed in Sec. IV. In particular, a hydration shell model[22,23] is discussed in that section. A discussion follows in Sec. V.

II. THEORETICAL DETAILS

We begin with a general form of the Smoluchowski equation[16] modified to include the effects of domain rotation and a spatially dependent sink within the two-domain model system:

$$\frac{\partial P(\mathbf{r},\Omega,t)}{\partial t} = [\nabla_{\mathbf{r}} \circ \mathbf{D} \cdot \nabla_{\mathbf{r}} + \nabla_{\Omega} \cdot \mathbf{R} \circ \nabla_{\Omega}] P(\mathbf{r},\Omega,t) + \frac{1}{k_B T} \nabla_{\mathbf{r}} \circ \mathbf{D} \cdot [P(\mathbf{r},\Omega,t) \nabla_{\mathbf{r}} U(\mathbf{r},\Omega)] + \frac{1}{k_B T} \nabla_{\Omega} \cdot \mathbf{R} \cdot [P(\mathbf{r},\Omega,t) \nabla_{\Omega} U(\mathbf{r},\Omega)] + K(\mathbf{r},\Omega) P(\mathbf{r},\Omega,t), \quad (1)$$

where $P(\mathbf{r},\Omega,t)$ is the time and spatial dependent probability that one domain exists separated from another and oriented relative to it. $K(\mathbf{r},\Omega)$ is an orientation dependent reaction operator that will be used to model the loss of encountering domains attributed to the coalescence process. $\mathbf{D}$ is the relative translational diffusion tensor, $\mathbf{R}$ is the rotational diffusion tensor, and $U(\mathbf{r},\Omega)$ is the potential energy affecting the rotational and relative translational diffusion.

The physical characteristics of the hypothetical protein domain system examined in this study follow closely from the two-particle orientation-dependent simulation of Zientara and Freed.[15] Figure 1 is a pictorial representation of the protein domain pair, whose mutual separation and relative orientation as a function of time are of interest. Each domain represents a region of local structure in the polypetide chain, that is, a contiguous section of the polypeptide chain that has adopted the same or similar local conformation as in the native state of the protein. These domains or nucleation centers for folding might be expected to involve such substructures as α-helices,[24] β-pleated sheets,[25] or hydrophobic cores.[26] (Compact domains in protein structures have recently been defined by Wodak and Janin[27] purely on the basis of surface area criteria.) In the actual protein, several nucleation sites might form in different parts of the polypeptide chain. The results obtained in this work reveal the mean observable time necessary for a pair of these domains to aggregate and form a larger coalesced region, which may either proceed to disaggregate or remain coalesced to become one permanent part of the protein's native tertiary structure.

For convenience in this effort to explore the simplest effects of domain–domain orientations and interactions, we assume in Eq. (1) that both domains can be described as spheres with hydrodynamic radii r_a and r_b located at two points along a flexible chain. This flexible chain represents the intervening polypeptide chain that connects the two domains. The spheres (i.e., domains) located along this chain translate independently in a solvent medium under the constraint of a maximum allowable separation. The motion of the domains is described by Brownian diffusion in three dimensions. At this step in our analysis we also choose to describe Ω dependent diffusion processes neglecting the effects of an intervening chain of finite size. Domain a is assumed to have spherically symmetric chemical properties and is chosen as the origin of the coordinate system within which relative translational diffusion will be represented. Domain b, whose orientation is specified by Euler angles, Ω, and whose rotation is governed by the diffusion tensor, $\mathbf{R}$, will now, for simplicity, be assumed to have a single preferred axis, $\mathbf{e}$. Therefore, one angle, θ, as seen in Fig. 1, is sufficient to account for the relevant orientation dependent domain interactions. This angle θ is the angle created by the intersection of $\mathbf{e}$ and the interdomain vector, $\mathbf{r}$, which is the axis connecting the domain centers. Also, we shall let $U(\mathbf{r},\Omega) = U(r)$ and $K(\mathbf{r},\Omega) = K(r,\theta)$ where $r = |\mathbf{r}|$ and $\mathbf{D} \to D\mathbf{1}$, and $\mathbf{R} \to R\mathbf{1}$ for simplicity. Suppressing all notation of φ in the following (its presence need only be included in later normalization factors), we can rewrite Eq. (1) to more explicitly define our model:

$$\frac{\partial P(r,\theta,t)}{\partial t} = \frac{D}{r^2} \frac{\partial}{\partial r} \left(r^2 \frac{\partial P(r,\theta,t)}{\partial r} \right) + \frac{(D/r^2 + R)}{\sin\theta} \frac{\partial}{\partial \theta} \sin\theta \frac{\partial P(r,\theta,t)}{\partial \theta} + \frac{1}{k_B T} \times \left[\frac{D}{r^2} \frac{\partial}{\partial r} \left(r^2 P(r,\theta,t) \frac{\partial U(r)}{\partial r} \right) \right] + K(r,\theta) P(r,\theta,t), \quad (2)$$

with the reflecting wall boundary conditions,

$$\left.\frac{\partial P(r,\theta,t)}{\partial r}\right|_{r=d} = \left.\frac{\partial P(r,\theta,t)}{\partial r}\right|_{r=r_N} = 0 \ , \tag{3}$$

which simulate the effect of having the domains linked by an intervening chain such that the distance of closest approach is $d = r_a + r_b$ and the greatest allowed separation is specified as r_N. These distance parameters d and r_N correspond to the distances a and b, respectively, utilized by earlier studies. Our analysis differs from that of others[1,28] in our use of the boundary conditions [Eq. (3)], functionally complicated force terms, and the spatially dependent reaction sink term $K(r,\theta)p(r,\theta,t)$ to simulate coalescence. This operator $K(r,\theta)$ also will be allowed to promote the formation of coalesced domains over a finite, but usually small, region of space. This more realistic[15,29] reaction representation is an improvement over the mathematically simpler domain contact forms required by analytical approaches. The relationship between the kinetic parameters used in our approach and those of Karplus and Weaver, who employed a Collins and Kimball[30] type partially absorbing inner boundary condition, has been discussed[29,31] previously and will be emphasized in the comparisons of results in Sec. III.[32] The coefficient $(D/r^2 + R)$ of the second term on the right-hand side of Eq. (2) demonstrates that a variation in θ can come about by the independent effects of translational motion (through the D/r^2 term) and by rotation of domain b, hence the R term.[29] The detailed derivation of these terms is given by Zientara and Freed,[15] who also point out the dimensionless ratio of interest,

$$Rd^2/D = 3r_a d/4\kappa_s r_b^2 \ , \tag{4}$$

which results from the Stokes–Einstein definitions,

$$D = \frac{k_B T}{6\pi\eta}\left(\frac{1}{r_a} + \frac{1}{r_b}\right) , \tag{5a}$$

$$R = \frac{k_B T}{8\pi\eta r_b^3 \kappa_s} \ , \tag{5b}$$

since $D = D_a + D_b$. Here, η is the bulk solvent viscosity, κ_s is a correction factor, which allows for the "rotational slip" of domain b, k_B is Boltzmann's constant, and T is the temperature.

An important question in any study involving the time-dependent orientational fluctuations of protein domains is whether both the translational and rotational portions of the second term of the right-hand side of Eq. (2) participate to the same degree in causing the relaxation of orientational preferences of the domains. Clearly, in physical systems of nonlinked diffusing particles[15] chemical effects due to rotational encounter mechanisms may be significant. These rotational chemical pathways may exert an influence on either the reactive[15,17-21] or quantum[15] aspects (or both) of certain diffusion-controlled systems. Referring to the protein model exhibited in Fig. 1, the assumed free-particle-like translational diffusion of each domain is rationalized by neglecting the finite bulk and rigidity of the intervening "chain," actually composed of amino acid residues. This fundamental protein backbone together with the side chains of the amino acids can also sterically inhibit translation by interdomain blocking intrusions. Indeed, the discrete nature of the protein segments separating domains may, for certain biochemical systems, possibly overcome simple diffusive stochastic behavior. However, we shall make the same assumption in this study as did Karplus and Weaver,[1] that is, the intervening polypeptide chain is unlikely to hinder the free translational diffusion of the domains. Effects of the connecting chain would be expected to become less significant as the length of the chain increases.

On the other hand, the completely free spherically symmetric rotational diffusion of any linked protein domain can be dismissed from consideration on intuitive grounds. In consideration of an intervening chain composed of discrete links rather than one resembling a flexible string, one may conjecture that an asymmetric (i.e., wobbling) rotation of the domain takes place about an axis formed by the adjacent rigid link of the interconnecting chain. This motion might exploit the domain's available rotational degree of freedom due to the single covalent bond linking the domain to the remaining protein segments. We shall ignore this possibility and assume in our numerical tests that the constraint of being located within the protein chain completely restricts the rotational character of domain b.[33] In this initial computational effort, therefore, we assume that the changes in relative orientation of the domain pair evolve solely through translational diffusion of the domains. This mechanism for protein microdomain coalescence is exhibited in Fig. 2.

Further simplifications of Eq. (2) can be attained first by the change of variable $\tilde{P}(r,\theta,t) = rP(r,\theta,t)$ and then by multiplication of both sides of the equation by the scaling factor d^2/D. The result of these changes is a new equation that includes dimensionless forms for all quantities: $y \equiv r/d$, $\tau = tD/d^2$, and $K(y,\theta) = K(r,\theta)d^2/D$. For computational ease we will perform all of our calculations after first applying the Laplace transform (to avoid the restriction of an iterative numerical scheme later), and employing the new probability variable,

$$\hat{P}(y,\theta,\sigma) \equiv \int_0^\infty e^{-\sigma\tau}\tilde{P}(y,\theta,\tau)\,d\tau \ . \tag{6}$$

In some of our analyses the domain system steady-state limit will be required. If necessary, it may be easily found from the $\tau \to \infty$ or $\sigma \to 0$ probability values.[29] A small but finite $\sigma < 10^{-10}$ usually suffices in these limiting cases.[34] As we shall note in the following, the calculation of the mean lifetimes of uncoalesced domains in different systems requires the use of any $1 \geq \sigma > 10^{-10}$.

The potential energy term in Eq. (2) will be treated as in earlier studies.[29,35] That is, we shall define the resulting force exerted by the domains on each other as

$$F(r) = -\frac{1}{k_B T}\frac{\partial U(r)}{\partial r} \ , \tag{7}$$

where the dimensionless forms are: $F(y) = dF(r) = \hat{F}(y)/y$ and $U(y) = U(r)/k_B T$. The force is defined such that $F(y) > 0$ describes a force causing an increase in the radial separation of the two domains. Consistent with this then, $U(y) > 0$ represents the interdomain repulsive

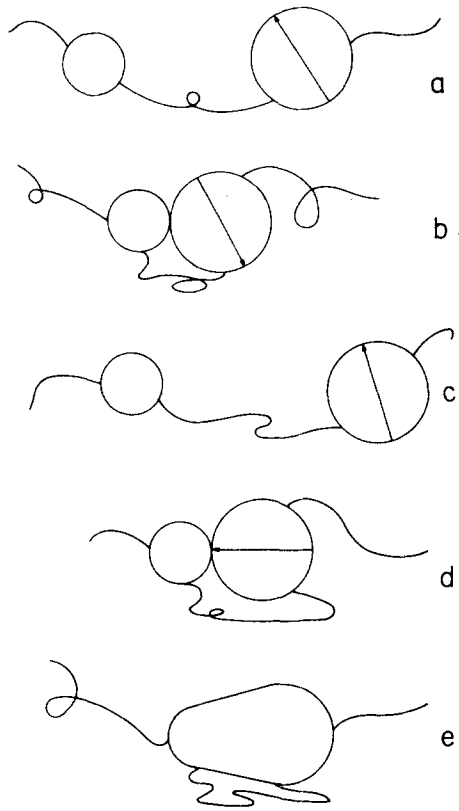

FIG. 2. Specific steps of the orientation dependent microdomain coalescence process as assumed in this study. (a) The protein domains are located at some initial separation. These domains result from the formation of near native conformations among nearby residues along the polypeptide chain. (b) Diffusion proceeds, affecting the domains, the intervening chain, and end chains. The domains approach, interact, and collide, possibly in a reactively unfavorable orientation. (c) The domains separate, diffusing apart while extending the intervening chain and simultaneously reorienting. (d) The domains approach, interact, and, in this example, collide in a reactively favorable orientation. (e) the coalescence product, a temporary or possibly permanent portion of the protein's native tertiary structure, is formed. In subsequent steps, this newly formed coalescence product may associate with a domain at another location along the polypeptide chain, coalesce, and result in the unique three-dimensional conformation of the native protein.

effects while $U(y)<0$ represents attraction.

These modifications allow us to rewrite Eq. (2) in a form readily inserted into the numerical scheme.

$$\sigma\hat{P}(y,\theta,\sigma)-\tilde{P}(y,\theta,0)=\frac{\partial^2\hat{P}(y,\theta,\sigma)}{\partial y^2}$$

$$+\frac{(1/y^2+Rd^2/D)}{\sin\theta}\frac{\partial}{\partial\theta}\left(\sin\theta\,\frac{\partial\hat{P}(y,\theta,\sigma)}{\partial\theta}\right)-\left(\frac{1}{y}\right)\frac{\partial}{\partial y}$$

$$\times[\hat{P}(y,\theta,\sigma)\hat{F}(y)]+K(y,\theta)\hat{P}(y,\theta,\sigma)\ . \tag{8}$$

We shall in our study choose the following first-order form to describe simply the orientation effects included in the specific reaction rate operator

$$K(y,\theta)=-[\kappa_0+\kappa_1(\tfrac{1}{2}+\tfrac{1}{2}\cos\theta)]\delta(y-1)\ , \tag{9}$$

where we can define for future use the isotropic and angular dependent portions as

$$\kappa'(y)\equiv(\kappa_0+\tfrac{1}{2}\kappa_1)\delta(y-1)\ , \tag{10a}$$

$$\kappa''(y,\theta)\equiv\tfrac{1}{2}\kappa_1(\cos\theta)\delta(y-1)\ , \tag{10b}$$

which will be employed in simulating domain coalescence (Fig. 2) in our numerical analysis. The Dirac delta function forms of Eqs. (10) duplicate exactly the contact type of reaction used by earlier studies.[1] Although the theoretical formulations are similar in this case and previous works, the application of these terms in our numerical scheme results in a finite extent of reactive region due to the spatial discretization of the numerical approximations.

We now expand $\hat{P}(y,\theta,\sigma)$ in a series of zero rank spherical harmonics, $Y_L^0(\theta,\varphi)$, according to

$$\tilde{P}(y,\theta,\tau)=\sum_{L=0}^{\infty}\tilde{P}^{(L)}(y,\tau)Y_L^0(\theta,\varphi)\ , \tag{11a}$$

$$\hat{P}(y,\theta,\sigma)=\sum_{L=0}^{\infty}\hat{P}^{(L)}(y,\sigma)Y_L^0(\theta,\varphi)\ , \tag{11b}$$

where the φ variable appears for completeness. The expansion in L can usually be truncated[15,36] at a value $L=L_{\max}$ such that convergence in the system's observed results has been obtained. For example, we can then write,

$$\hat{P}(y,\theta,\sigma)\cong\sum_{L=0}^{L_{\max}}\hat{P}^{(L)}(y,\sigma)Y_L^0(\theta,\varphi) \tag{12}$$

and perform test calculations to insure that the truncation error is negligible. This simplifies greatly the method of solution of Eq. (8) because the spherical harmonics form the orthonormal eigenfunctions of the rotational diffusion operator, with eigenvalues equal to $L(L+1)$. We can take advantage of this feature by introducing in Eq. (8) the $\hat{P}(y,\theta,\tau)$ and $P(y,\theta,\tau)$ forms utilizing the expansion of Eq. (12). Multiplying the resulting equation by $Y_L^0(\theta,\varphi)$ and integrating over all allowed values of θ, $0\le\theta\le\pi$, and φ, $0\le\varphi\le2\pi$, yields an equation governing the y and σ dependence of the probability coefficients,

$$\sigma\hat{P}^{(L)}(y,\sigma)-\tilde{P}^{(L)}(y,\sigma)=\frac{\partial^2\hat{P}^{(L)}(y,\sigma)}{\partial y^2}$$

$$+\left(\frac{1}{y^2}+\frac{Rd^2}{D}\right)L(L+1)\hat{P}^{(L)}(y,\sigma)-\frac{1}{y}\frac{\partial}{\partial y}[\hat{P}^{(L)}(y,\sigma)\hat{F}(y)]$$

$$+\sum_{L'=0}^{L'_{\max}}\hat{P}^{(L')}(y,\sigma)\left(\int_0^{2\pi}\int_0^{\pi}Y_L^0K(y,\theta)Y_{L'}^0\sin\theta\,d\theta\,d\varphi\right)\quad\text{for all } L=0,\ 1,\ \ldots,\ L_{\max} \tag{13}$$

where we note the solution of Eq. (13) requires the integrals

$$\int_0^{2\pi}\int_0^{\pi} Y_L^0(\theta,\varphi)(\cos\theta)Y_{L'}^0(\theta,\varphi)\sin\theta\,d\theta\,d\varphi = \frac{-L}{[(2L-1)(2L+1)]^{1/2}} \equiv L^+ \quad \text{for } L' = L-1$$

$$= -\frac{(L+1)}{[(2L+1)(2L+3)]^{1/2}} \equiv L^- \quad \text{for } L' = L+1 \tag{14a}$$

and the orthonormality condition

$$\int_0^{2\pi}\int_0^{\pi} Y_L^0(\theta,\varphi)Y_{L'}^0(\theta,\varphi)\sin\theta\,d\theta\,d\varphi = \delta_{L,L'} \ . \tag{14b}$$

From Eq. (13) we wish to note the coefficient [i.e., $\hat{P}^{(L)}(y,\sigma)$] coupling caused by an asymmetric domain's "reactivity" or coalescence. The last term of the right-hand side of Eq. (13) consisting of integrals involving the reaction operator, $\kappa(y,\theta)$, may possibly couple coefficients with $L' \neq L$ by virtue of Eqs. (10b) and (14a). The translational diffusion terms are seen to couple only values of the probability coefficients with identical L values. The rotational diffusion operator, although coupling only similar L value coefficients, causes the exponential decay of the nonzero L value coefficients. This is the appearance of the origin of the mechanism of orientational relaxation in our domain pair system. This process will, for example, cause the eventual randomization in the orientational distribution of initially anisotropically oriented domains. Also, it will provide the reason for the orientational relaxation of a system whose probability θ-profile has become nonuniform due to the angular specific coalescence of domains during a domain pair encounter.

The orientational relaxation process can be described by the decay of any preferred state of the angular description of domain–domain location relative to the r axis. We can associate this decay with an effective dimensionless time parameter[15] [cf. Eq. (13)] that is a function of interdomain separation:

$$\tau_{R\,eff}^{*}(y)^{-1} = \tau_R^{*-1} + \tau_T^{*}(y)^{-1} \ , \tag{15}$$

where the dimensionless rotational correlation time is

$$\tau_R^{*-1} \equiv \frac{1}{6}\left(\frac{Rd^2}{D}\right)^{-1} = \frac{2}{9}\frac{\kappa_s r_b^2}{dr_a} \tag{16}$$

and the dimensionless characteristic time associated with a translational displacement of $(\Delta y)^2$ in three-dimensional liquids is[37]

$$\tau_T^{*}(\Delta y) \equiv \tfrac{1}{6}(\Delta y)^2 \ . \tag{17}$$

By our arguments above, we will assume a negligible rotational contribution to the relaxation mechanism, i.e., $\tau_R^{*-1} \cong 0$.

The relevant observable quantities regarding time (or σ) dependent coalescence yield can be calculated using the definition of Eq. (12). Thus, the probability that the domain pair in the studied system remains uncoalesced[38] for a given value of σ is

$$\hat{\mathcal{P}}(\sigma) \equiv \sigma\mathcal{P}(\sigma) = \sigma\int_1^{y_N}\int_0^{2\pi}\int_0^{\pi} Y_0^0(\theta,\varphi) \times \hat{P}(y,\theta,\varphi,\sigma)\,y\sin\theta\,d\theta\,d\varphi\,dy \ , \tag{18}$$

where the Jacobian entering in Eq. (18) is modified by our earlier transform of $P \to \tilde{P}$. The uncoalesced domain probability in the steady-state limit can, again, be found via $\mathcal{P} \equiv \lim_{\sigma\to 0}\sigma\mathcal{P}(\sigma)$. We can then define the reaction or coalescence product yield via equations analogous to Eq. (18),

$$\sigma\mathcal{F}(\sigma) \equiv 1 - \hat{\mathcal{P}}(\sigma) \ , \tag{19a}$$

and in the steady state,

$$\mathcal{F} \equiv 1 - \mathcal{P} \ . \tag{19b}$$

To obtain the mean lifetime of the uncoalesced domain pair within the specific system under study, we will assume that a single decay time, τ^*, governs the yield, $\sigma\mathcal{F}(\sigma)$, via

$$\mathcal{F}(\sigma) = \frac{\tau^{*-1}}{\sigma(\sigma+\tau^{*-1})} \ , \tag{20}$$

which has the appropriate Laplace inverse,

$$\mathcal{F}(\tau) = 1 - e^{-\tau/\tau^*} \ . \tag{21}$$

By definition,[1,28] the mean lifetime is the first moment of the time variation of the product yield

$$\tau(\text{mean lifetime}) = \int_0^{\infty} t\left(\frac{d\mathcal{F}(t)}{dt}\right)dt = \left(\frac{\tau^* d^2}{D}\right) \ . \tag{22}$$

In other words, the quantity τ^* calculated from a numerical solution of Eq. (13) is the required dimensionless form of the mean lifetime of uncoalesced domain pairs. The inverted form of Eq. (20) will be used in obtaining our results,

$$\tau^* = [1 - \sigma\mathcal{F}(\sigma)]/[\sigma^2\mathcal{F}(\sigma)] \ . \tag{23}$$

Numerical tests were performed for validation purposes throughout the σ spectrum and $\mathcal{F}(\sigma)$ was fit to Eq. (20). Negligible (<1%) error in τ^* resulted indicating that the assumption of a single system relaxation time is indeed applicable in *both* situations where forces between the domains were either absent or present. In Sec. III we shall discuss the numerical method utilized in the solution of Eq. (13) and the calculations leading to the result of Eq. (23). In Sec. IV we will present results based on calculations of τ^* from Eq. (23) and $\mathcal{F}(\sigma)$ values calculated by numerical means.

III. NUMERICAL METHOD

The solution of Eq. (13) involves additionally a treatment of the remaining domain separation variable y. Once values for the coefficients, $\hat{P}^{(L)}(y,\sigma)$ [and thus $\hat{P}(y,\sigma,\theta)$] are obtained for some chosen σ value, the probability of domains within the system, $\hat{\mathcal{P}}(\sigma)$, can be calculated by Eq. (18), $\mathcal{F}(\sigma)$ via Eq. (19a), and ultimately τ^* using Eq. (23). The first step in this solution leads us to treat the y dependence in Eq. (13) by the

method of finite differences (FD).[15,29] In implementing this method, the independent variable y and the variables dependent on y will be specified only at discrete nodes (i.e., node 1 to node N) in space, with the nodal index designated through the subscript. For example, the spatial nodes (connecting concentric shells of infinitisimal thickness) will be fixed at the distances y_i where $1 \le i \le N$. The entire region available to the diffusing domains consists of an inner region where $1 \le y \le 1+\Delta_I$ and the remaining diffusion space of $1+\Delta_I \le y \le y_N$, such that

$$y_1 = 1 , \tag{24a}$$

$$y_2 = 1 + \Delta_I , \tag{24b}$$

and

$$y_i = 1 + \Delta_I + (i-2)\Delta \quad \text{for } 2 \le i \le N , \tag{24c}$$

where Δ is a fixed chosen FD nodal separation quantity. This permits us to specify the extent of the reactive region (as $1 \le y \le \frac{1}{2}\Delta_I$) where the reactive (i.e., sink) terms cause the reduction of the uncoalesced domain population. The important model parameter, the greatest allowed domain center separation, is, from Eq. (24c),

$$y_N = 1 + \Delta_I + (N-2)\Delta . \tag{25}$$

Thus, the radial range of the diffusion space excluding the finite size of the domains is $y_N - 1$ corresponding to $(b-a)/l$ of Karplus and Weaver.[1]

Following the nodal specification of the radial separation variable, we can now write in FD terms the dimensionless dependent variables from Eq. (13) as $\hat{P}^{(L)}(y_i, \sigma)$, $\hat{F}(y_i)$, and $K(y_i, \theta)$. This notation is further simplified by $\hat{P}^{(L)}(y_i, \sigma) \to \hat{P}^{(L)}(i, \sigma)$, $\hat{F}(y_i) \to \hat{F}(i)$ and $K(y_i, \theta) \to K(i, \theta)$. The translational diffusion operator, which couples the probabilities at two nodes, can be written in a FD scheme by using Eq. (24) and the methods outlined in Refs. 15 and 34. This yields the elements of the transition matrix, $\mathbf{W}$, which comprise the FD analog of the Smoluchowski diffusion operator. The elements of the tridiagonal matrix $\mathbf{W}$ are:

$$W_{1,1} = -2(1+\Delta_I)/(\Delta_I)^2 - F(2)(1+\Delta_I)/\Delta_I , \tag{26a}$$

$$W_{1,2} = 2/(\Delta_I)^2 - F(1)/\Delta_I , \tag{26b}$$

$$W_{2,1} = 2/[\Delta_I(\Delta+\Delta_I)] + F(2)/(\Delta_I+\Delta) , \tag{26c}$$

$$W_{2,2} = -\frac{2}{(\Delta_I\Delta)} - \frac{[F(3)(1+\Delta_I+\Delta) - F(1)]}{[(1+\Delta_I)(\Delta_I+\Delta)]} , \tag{26d}$$

$$W_{2,3} = 2/[\Delta(\Delta_I+\Delta)] - F(2)/(\Delta_I+\Delta) , \tag{26e}$$

and, for $3 \le i \le (N-1)$,

$$W_{i,i-1} = 1/\Delta^2 + F(i)/(2\Delta) , \tag{27a}$$

$$W_{i,i} = -2/\Delta^2 - \frac{[F(i+1)y_{i+1}/y_i - F(i-1)y_{i-1}/y_i]}{(2\Delta)} , \tag{27b}$$

$$W_{i,i+1} = 1/\Delta^2 - F(i)/(2\Delta) , \tag{27c}$$

and, finally,

$$W_{N,N-1} = 2/\Delta^2 + F(N)/\Delta , \tag{28a}$$

$$W_{N,N} = -2(1-\Delta/y_N)/\Delta^2 + F(N-1)[(1-\Delta/y_n)/\Delta] , \tag{28b}$$

with all other $W_{i,j} = 0$ for $j \ne i$ or $i \pm 1$. Note here for ease we have written Eqs. (26)–(28) employing the actual dimensionless force, $F(i)$, rather than $\hat{F}(i)$.

As in Ref. 15, we can order the probability coefficients, $\hat{P}^{(L)}(i, \sigma)$ and construct a supervector

$$\hat{\mathbf{P}}(\sigma) \equiv \begin{pmatrix} \hat{\mathbf{P}}(1,\sigma) \\ \hat{\mathbf{P}}(2,\sigma) \\ \vdots \\ \hat{\mathbf{P}}(N,\sigma) \end{pmatrix} , \tag{29}$$

where each subvector contains $(L_{\max}+1)$ elements written as,

$$\hat{\mathbf{P}}(i,\sigma) \equiv \begin{pmatrix} \hat{P}^{(0)}(i,\sigma) \\ \hat{P}^{(1)}(i,\sigma) \\ \vdots \\ \hat{P}^{(L_{\max})}(i,\sigma) \end{pmatrix} . \tag{30}$$

$\tilde{\mathbf{P}}(\tau)$ is created in the same fashion as its Laplace transform in the preceding in Eqs. (29) and (30).

When all operators from the right-hand side of Eq. (13) are likewise included with $\mathbf{W}$ in coupling the elements of $P(\sigma)$, there results a supermatrix[15,34–36] structure that is arranged and written in matrix form as

$$\mathbf{A}\hat{\mathbf{P}}(\sigma) = \tilde{\mathbf{P}}(\tau = 0) , \tag{31}$$

where $\mathbf{A}$ is block tridiagonal (i.e., $\mathbf{A}_{i,j} \ne 0$ for $j = i$, $i \pm 1$) and the submatrices are given by

$$\mathbf{A}_{i,i\pm1} = -W_{i,i\pm1} \times \mathbf{1} \tag{32}$$

where $\mathbf{1}$ being the unit matrix of dimension $(L_{\max}+1)$ and $W_{i,j}$ is the ijth element of the transition matrix.

From Eq. (10) and using our FD notation we can write the terms of the reaction (i.e., coalescence) operator as

$$\kappa'(i) \equiv \kappa'(y_i) = (\kappa_0 + \tfrac{1}{2}\kappa_1)\delta_{i,1} , \tag{33a}$$

$$\kappa''(i) = \tfrac{1}{2}\kappa_1 L^{\pm}\delta_{i,1}\delta_{L,L\pm1} . \tag{33b}$$

Likewise, the rotational terms of Eq. (13) can be described through the FD operator

$$\hat{W}_{i,i} \equiv (1/y_i^2 + Rd^2/D) . \tag{34}$$

The final block diagonal submatrices of $\mathbf{A}$ can now be constructed. Using the simplifying notation $\mathbf{A}_{i,i} \to \mathbf{A}^{(i)}$ to retain an indicator of nodal index then we can define the elements of each tridiagonal $\mathbf{A}^{(i)}$ as

$$A^{(i)}_{l,l} = \sigma - W_{i,i} + \kappa'(i) - l(l+1)W_{i,i} \tag{35a}$$

and

$$A^{(i)}_{l,l\pm1} = \tfrac{1}{2}\kappa_1\delta_{i,1}L^{\pm} \tag{35b}$$

for $l = 0$ to $L_{\max}$ with all other $A^{(i)}_{l,m} = 0$. The definitions of L^+ and L^- are given earlier in Eq. (14a).

For solution we need only perform a single matrix inversion to calculate the coefficients of the spherical harmonics as seen in Eq. (12). That is, for some finite positive value of σ,

$$\hat{\mathbf{P}}(\sigma) = \mathbf{A}^{-1}\tilde{\mathbf{P}}(\tau = 0) . \tag{36}$$

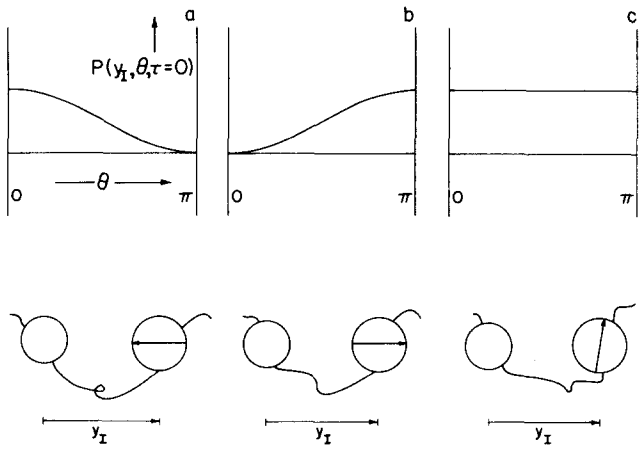

FIG. 3. Graphic and pictorial representations of the initial conditions of domein orientation utilized in this study. (a) $P(y_I, \theta, \tau=0) \propto (1+\cos\theta)$, with most domains oriented such that $\theta \cong 0$. The case of domains oriented with $\theta = 0$ is depicted above; (b) $P(y_I, \theta, \tau=0) \propto (1-\cos\theta)$, with most domains oriented such that $\theta \cong \pi$. The case of domains oriented with $\theta = \tau$ is depicted above; (c) $P(y_I, \theta, \tau=0) =$ constant, with a completely random domain orientation. One possible orientation is pictured having $0 < \theta < \tau$.

Then, from Eq. (18) written in FD terms the probability that uncoalesced domains still exist is calculated using

$$\hat{\mathcal{P}}(\sigma) = \sigma \sum_{i=1}^{N} \hat{P}^{(0)}(i, \sigma) V(i) , \tag{37}$$

where only the $L=0$ coefficients contribute as expected and the FD volume elements, $V(y_i) \rightarrow V(i)$, are the analogs of the continuous differential $y\,dy$, written as

$$V(1) = \tfrac{1}{2}\Delta_I , \tag{38a}$$

$$V(2) = (\Delta_I + \Delta)/[2(1+\Delta_I)] , \tag{38b}$$

$$V(i) = y_i\,\Delta \quad \text{for } 3 \le i < N , \tag{38c}$$

and

$$V(N) = \tfrac{1}{2} y_N\,\Delta . \tag{38d}$$

The value of $\hat{\mathcal{P}}(\sigma)$ from Eq. (32) is then used to compute $\sigma\mathcal{F}(\sigma)$ via Eq. (19a), after which τ^* is found using Eq. (23). Only one matrix inversion is necessary provided results are based on a small but finite value of σ and $\sigma > 0$. This is because Eq. (23) yields τ^* irrespective of the σ value used; thus we have uniformly utilized $\sigma = 10^{-8}$ in our numerical calculations, except as noted.

An important factor in the analysis of protein folding is the correct specification of an initial condition that reveals the correct original orientation of the diffusing domains. This is easily implemented using the computational method described previously. In Sec. IV we shall employ two specific initial conditions where the domains exhibit an orientational preference, plus the case of an isotropic initial condition. These different cases can be seen in Fig. 3, which exhibits a particular situation where the domains start at an initial center-to-center separation y_I.

For the example of a uniform spatial distribution in the initial condition which is also isotropically oriented,

$$P(r, \theta, \tau=0) = \left(\frac{1}{4\pi}\right)^{1/2} , \tag{39a}$$

which can be applied in Eqs. (31) and (36) in dimensionless terms through the equivalent statement:

$$\tilde{P}^{(0)}(i, \tau=0) = y_i/N , \tag{39b}$$

and

$$\tilde{P}^{(L)}(i, \tau=0) = 0, \quad \text{for } L > 0 \tag{39c}$$

where the y_i factor occurs due to the earlier change of variable. The two simple cases of anisotropic initial conditions[15] we shall study are specified by

$$P(r, \theta, \tau=0) = \left(\frac{1}{4\pi}\right)^{1/2} (1 \pm \cos\theta) \tag{40a}$$

or, in FD terms,

$$\tilde{P}^{(0)}(i, \tau=0) = y_i/N \tag{40b}$$

and

$$\tilde{P}^{(1)}(i, \tau=0) = (\pm 1/\sqrt{3})(y_i/N) \tag{40c}$$

with

$$\tilde{P}^{(L)}(i, \tau=0) = 0 \quad \text{for } L > 1 \tag{40d}$$

where the $(\pm)$ options in Eq. (40c) refer to the choices of the respective initial condition θ-probability profile in Eq. (40a). The modification of the preceding values to denote a specific starting domain separation, for example at y_I, involves the multiplication of Eqs. (39a) and (40a) by $\delta(r - r_I)$ noting $y_I = r_I/d$. Then Eq. (39b) becomes

$$\tilde{P}^{(0)}(i, \tau=0) = y_I \delta_{i,I} \tag{41}$$

and in the case of anisotropic initial conditions Eqs. (40b) and (40c) become

$$P^{(0)}(i, \tau=0) = y_I\,\delta_{i,I} , \tag{42a}$$

$$P^{(1)}(i, \tau=0) = (\pm 1/\sqrt{3})(y_I\,\delta_{i,I}) . \tag{42b}$$

Computations were carried out using a PDP 11/34 minicomputer. The matrix inversion of Eq. (36) was accomplished in each case by Gaussian elimination with partial pivoting.

IV. RESULTS FOR COALESCENCE LIFETIMES

A. In the absence of forces

The approximate analytic results of Karplus and Weaver[1] and Adam and Delbrück[28] were used to determine the accuracy of our numerical approach. In all the different physical models studied using our numerical methods (i.e., force free or forces present, cases I–IV) tests for the convergence of the results were performed to optimize the numerical parameters N and L_{max}. These tests revealed the numerical results quoted to be in most cases $< 1\%$ in error due to the FD discretization and L truncation approximations, except the results for the hydration shell model (Sec. IV B, Case IV) are qualified to be $< 5\%$ in error due to the large magnitude and spatial variation of the assumed forces. For domains in three-dimensional isotropic diffusion space and a weakly absorbing coalescence process, we

can write in our notation the formula of Karplus and Weaver for the dimensionless mean lifetime of uncoalesced domains (with a spatially uniform and isotropic initial condition) as[39]

$$\tau^* = \left(\frac{2}{\kappa_{eff}\,\Delta_I}\right)\left(\frac{y_N^3 - 1}{3}\right), \quad \text{for } \kappa_{eff} \ll 1 , \tag{43}$$

where we have introduced an effective spherically symmetric reaction rate constant that is a function of our orientation dependent reaction parameters,[15]

$$\kappa_{eff} \equiv \kappa_0 + \tfrac{1}{2}\kappa_1 \tag{44}$$

with κ_0 and κ_1 entering the numerical problem through Eq. (33). In Eq. (43) this effective specific rate constant (times $\frac{1}{2}\Delta_I$) enters in place of Karplus and Weaver's β absorption factor. This is due to the pseudo-first-order reaction process[29] we utilize to simulate coalescence. The use of this process in our calculations allows the coalescence of domains in the radial region $1 \le y \le 1 + \frac{1}{2}\Delta_I$, thus the additional appearance of this distance term. In contrast, the Collins and Kimball[30] boundary condition employed by Karplus and Weaver permits coalescence only on actual domain contact, a hard-sphere technique. Table I is a comparison of results for this force free case indicating <1% error in our numerical results in weakly absorbing examples.

Also in Table I we compare our results in the limit of complete absorption (i.e., the domains have unit probability of coalescing after coming in contact) to the approximate formula of Adam and Delbrück[28] (which they note as having <2% error for $y_N \ge 10$) written as

$$\tau^* \cong \tfrac{1}{3} y_N^3 (1 - 1/y_N)^2 \quad \text{for } \kappa_{eff} \gg 1 . \tag{45}$$

TABLE I. τ^*, mean lifetimes of uncoalesced domains, in the absence of forces. Results for $P(y, \theta, \tau = 0) = \text{constant}$, in a case of weak absorption and the complete absorption limit.[a]

$(y_N - 1)$[b]	$\kappa_1 = 10^{-5}$ Weak absorption[c]	$\kappa_1 = 10^6$ Complete absorption[d]
1	9.33×10^6 (9.33×10^6)	6.43×10^{-1} (6.66×10^{-1})
5	2.87×10^8 (2.87×10^8)	4.42×10^1 (5.00×10^1)
10	1.77×10^9 (1.77×10^9)	3.29×10^2 (3.67×10^2)
20	1.23×10^{10} (1.23×10^{10})	2.57×10^3 (2.80×10^3)
100	1.37×10^{12} (1.37×10^{12})	3.22×10^5 (3.37×10^5)

[a]Finite difference results found using the input as noted together with $\kappa_0 = 0$, $\Delta_I = 0.1$, $L_{max} = 4$, and an isotropic, spatially uniform initial condition. Additional input of $N = 51$ and $\tau_R^* = 16.67$ was used in the case of weak absorption. $N = 100$ and $\tau_R^* = 0$ were used to study complete absorption.

[b]The finite difference spatial discretization value employed, Δ, can be calculated for each case from Eq. (25) and the above imput.

[c]The numerical result is listed first, with the value calculated from the result of Karplus and Weaver (Ref. 1), given in Eq. (43), following in parentheses.

[d]The numerical result is listed first, with the value calculated from the approximate formula derived by Adam and Delbrück (Ref. 28), Eq. (45) of this work, following in parentheses. Numerical results were found utilizing the input noted above except $\kappa_1 = 10^8$ differed by <1% from the results displayed above for $\kappa_1 = 10^6$.

TABLE II. τ^*, mean lifetimes of uncoalesced domains, in the absence of forces. Results for $P(y, \theta, \tau = 0) = \delta(y - y_I)$.[a]

y_I	κ_1[b] $= 10$	10^3	10^6[c]
1.826	1.14×10^4	5.04×10^2	2.01×10^2 (2.00×10^2)
3.864	1.16×10^4	6.30×10^2	3.27×10^2 (3.27×10^2)
5.903	1.16×10^4	6.67×10^2	3.63×10^2 (3.63×10^2)
7.942	1.16×10^4	6.81×10^2	3.78×10^2 (3.77×10^2)
11.000	1.16×10^4	6.87×10^2	3.84×10^2 (3.83×10^2)

[a]Finite difference results found using the input $N = 100$, $L_{max} = 4$, $y_N = 11$, $\Delta_I = 0.01$, $\tau_R^{*-1} = 0$, $\kappa_0 = 0$, and an isotropic initial condition, with unit probability at location $y = y_I$ and zero elsewhere.

[b]Results utilizing a reactivity $\kappa_{eff} \le 1$ exhibit <1% variation in τ^* for $1.826 \le y_I \le 11$ with other input similar to that preceding.

[c]The numerical result is listed first for input of $\kappa_1 = 10^6$ with the value calculated from the result of Weaver (Ref. 40), Eq. (46) of this work, following in parentheses.

Our results, which apply to a range in y_N beyond the limits for which Eq. (45) can be used show about 10% deviation from values calculated from Eq. (45). As noted in Table I we have chosen the isotropic portion of the reactivity, κ_0, to equal zero in our calculations. The angular dependence of the reactivity in this case, $\kappa(y, \theta) \propto (1 + \cos\theta)$ (cf. Fig. 2 of Ref. 15), more appropriately describes protein domains that coalesce in a preferred orientation (i.e., an orientation where $\theta \cong 0$). Because of orientational relaxation on the time scale of $\tau_{R\,eff}^*$ we have not observed particular orientation dependent effects arising from domains initially in an isotropic spatially uniform distribution other than the reduction in domain reactivity through Eq. (44). Indeed, results calculated in these cases by simple isotropic methods, using κ_{eff} given by Eq. (44) differ by <5%. These two methods yield almost exactly the same results in cases of low reactivity, $\kappa_{eff} \ll 1$. This is due to the need for repeated domain encounters that cause ample orientational relaxation during diffusive excursions and an almost completely isotropic domain distribution prior to experiencing a new opportunity for coalescence. These observations are only true, in general, for isotropic initial conditions. As we shall see in the following, anisotropic initial conditions will produce a significant orientation dependent effect on the mean lifetime of uncoalesced protein domains, particularly when the total allowed domain separation, y_N, is small.

The extent of the accuracy of our numerical results in the complete absorption limit was further tested in the case of a specific initial domain separation. This case was recently analyzed by Weaver.[40] Table II illustrates the variation in lifetimes for different values of the initial domain separation, y_I. In the complete absorption limit ($\kappa_{eff} \gg 1$), our results vary by <1% (as y_I varies an order of magnitude) from those calculated from Weaver's exact analytic formula,

$$\tau^* = \tfrac{1}{6}(1 - y_I^2) + \tfrac{1}{3} y_N^3 (1 - 1/y_I) \quad \text{for } \kappa_{eff} \gg 1 . \tag{46}$$

However, results were obtained for the complete range of effective reactivities, κ_{eff}, from which we have ob-

TABLE III. τ^*, mean lifetimes of uncoalesced domains in the absence of forces. Results for anisotropic initial conditions.[a]

κ_1	$P(y,\theta,\tau=0)$ $(4\pi)^{-1/2}(1+\cos\theta)\delta(y-y_I)$	$P(y,\theta,\tau=0)$ $=(4\pi)^{-1/2}(1-\cos\theta)\delta(y-y_I)$	Isotropic initial condition: $P(y,\theta,\tau=0)=\delta(y-y_I)$
10^{-5}	1.77×10^{10}	1.77×10^{10}	1.77×10^{10}
10	1.36×10^{4}	9.65×10^{3}	1.16×10^{4}
10^{3}	6.49×10^{2}	7.26×10^{2}	6.87×10^{2}
10^{5}	3.87×10^{2}	3.88×10^{2}	3.87×10^{2}
10^{6}	3.84×10^{2}	3.84×10^{2}	3.84×10^{2}

[a]Finite difference results found using the input values $N=100$, $L_{max}=4$, $y_N=11$, $\Delta_I=0.01$, $\tau_R^{*-1}=0$, $\kappa_0=0$, $y_I=11$, and the specific initial condition as noted.

served for $\kappa_{eff} \lesssim 10$ that $\tau^* \propto (\kappa_{eff})^{-1}$ and $\tau^* \neq f(y_I)$.

When we analyzed the variation in the mean lifetimes of the uncoalesced domains versus the reactivity (or coalescence ability) for the anisotropic initial conditions discussed in the preceding and noted by Eqs. (41) and (42). This comparison is seen in Table III and the specific initial conditions are described in detail in Fig. 3.

As observed in Table III the values for τ^* are independent of the preferred initial domain orientation in both the $\kappa_{eff} \to 0$ and $\kappa_{eff} \to \infty$ limits. This can be explained in the first case by the long periods of diffusive walks during which orientational relaxation occurs. eliminating any possible anisotropic initial condition effects. This orientational relaxation takes place in a time $\tau^*_{R\,eff}$ which can be calculated from Eq. (15) and the input listed in Table III. For example, if $y_N=11$ and $\tau_R^{*-1}=0$, then $\tau^{*\,(y)}_{R\,eff}=\tau^*_T(y)$. This yields the value for the effective relaxation time $\tau^*_{R\,eff} \gtrsim 20.2$ [for $\tau^*_T(y_N)$ from Eq. (17)] so for weakly absorptive reactivities $\tau^*_{R\,eff} \ll \tau^*$. We note that $\tau^*_{R\,eff}$ is on the short time scale of the mean lifetimes observed for complete absorption. It follows, then, that orientation dependent effects may be permitted by this argument for the case of complete absorption. In this special case, however, the domains exist in the reactive or coalescence region long enough to allow them to reorient and coalesce without requiring additional encounters. This is the predominant factor that quenches any effects of an anisotropic initial condition in these circumstances.

B. Forces present

Proteins are composed of long chains of amino acid residues linked by peptide bonds. In solution a polypeptide chain in the absence of any form of stabilizing interactions would tend to produce a tangled string in continuous conformational flux, i.e., a random coil.[41] However, the native state, exhibiting a unique, stable three-dimensional structure, is known to be attained spontaneously from the amino acid sequence under proper environment.[2,3] The forces responsible for the formation and maintenance of the native conformation must be able to overcome the configurational entropy of the disordered form. The major types of interactions that cooperate in stabilizing the native tertiary structure of a globular protein include hydrogen bonds between peptide groups or between various amino acid side chains, hydrophobic bonds between nonpolar residues, and ionic bonds between positively and negatively charged side chains. (Disulfide bonds, which covalently link different segments of the polypeptide chain, are only regarded as a means of added stability in those proteins in which they occur, leaving the noncovalent interactions left to account for protein folding).[2,41] In the present study we will incorporate the presence of several types of forces and examine the effects on the mean coalescence time τ^*, for two spherical domains, to simulate the interactions present in a folding polypeptide chain.

The Smoluchowski equation, as applied in this problem [cf. Eq. (1)], includes the effects of a spatially varying potential energy for two diffusing particles, that is, the protein domains. Through Eq. (8), we have shown how the potential energy, and hence the interdomain forces, can be included in the theoretical analysis of domain coalescence and the mean lifetimes of uncoalesced domain pairs. However, the solution of this biochemical problem and other problems in chemical physics utilizing the Smoluchowski or stochastic Liouville[29] equations including complicated potentials clearly requires numerical methods[29,42] since analytic mathematical solutions to the underlying equations do not exist.

In the discussion that follows we shall study the effects of four forms of spatially varying domain–domain interactions. In the first three cases the functional form of the potential energy employed may represent ionic solvent effects on charged domains or may be generalized from the examples noted to account for nonionic domain interactions, which may be simulated by similar potential energy functions. Positively and negatively charged groups such as the $-NH_3^+$ of lysine residues and the $-COO^-$ of aspartic and glutamic acid residues would account for charges on the protein domains. The source of nonionic energy variations could be, for example, an approximation to the non-negligible effects of the intervening chain and its finite size or solvent excluded-volume effects. The final case, which will be discussed separately, simulates the effects of hydrophobic interactions and is based on the hydration shell model of Nemethy and Scheraga.[43] The energetics

of this reflect the requirement of the domains to penetrate each other's hydration shell (or layer) before coalescence.

All of the potential energy functions (and respective forces) included in our numerical approach can be defined either as continuous (as in the following) or discontinuous[35] functions, or they may exist only numerically [and the nodal values input directly to Eqs. (26)–(28)]. The first three cases of domain–domain interactions to be studied are the following.

Case I. Debye-Hückel ionic interaction (Ref. 44)

$$U(y) \equiv \left(\frac{Z_a Z_b e^2}{\epsilon d k_B T}\right) \frac{\exp[-\kappa_{DH} d(y-1)]}{y(1+\kappa_{DH} d)} \quad . \tag{47}$$

Case II. Exponentially decaying interaction

$$U(y) \equiv \left(\frac{Z_a Z_b e^2}{\epsilon d k_B T}\right) \exp\left(\frac{-y}{y_E}\right) \quad . \tag{48}$$

Case III. Coulombic interaction

$$U(y) \equiv \left(\frac{Z_a Z_b e^2}{\epsilon d k_B T}\right) \frac{1}{y} \quad . \tag{49}$$

Z_a and Z_b are the effective electrical charges (carrying the sign) of the two domains; e, the fundamental electronic charge ($=4.802\,86\times10^{10}$ esu); ϵ, the dielectric constant of the medium; k_B, the Boltzmann constant; T, temperature in degrees Kelvin; κ_{DH}, inverse of the Debye length[44]; and y_E, a characteristic length for the exponentially decaying potential energy example, We can note from the earlier discussion of this section that the relevant variables of the coalescence process are y_N, κ_0, κ_1, Δ_I. and possibly y_I. In the following studies of model interactions we will choose certain experimentally applicable examples of system parameters as our basis and only observe the effects of the magnitude and functional form of the domain–domain interactions.

The overall structure of a folded protein is remarkably compact.[2] For example, the extended polypeptide chain with 58 residues of bovine pancreatic trypsin inhibitor has a length of 211 Å (3.63 Å/residue), yet the folded state has a maximum dimension of 29 Å.[45] In the case of a larger protein, the extended chain of carboxypeptidase, with 307 residues would be 1114 Å long, but the maximum dimension of the folded molecule is only about 50 Å.[46] Since the folded state of large proteins seems to be divided into several relatively independent domains the choice of $d=10$ Å for the diameter of one such domain therefore seems reasonable and consistent with known protein dimensions.

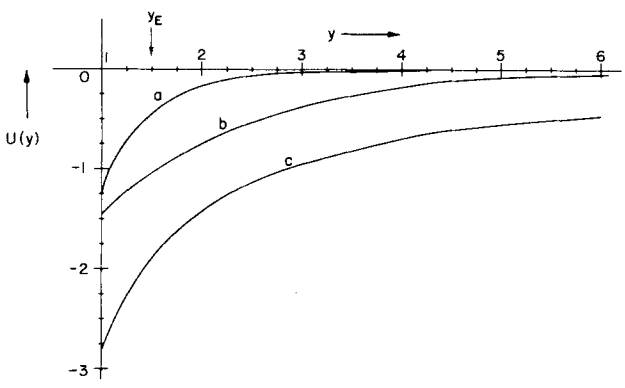

FIG. 4. Potential energy vs interdomain separation for examples of cases I–III. Curve *a* includes Debye–Hückel type ionic effects, the energy calculated using Eq. (47) and $\kappa_{DH} d = 1.272$. Curve *b* corresponds to an exponentially decaying potential energy calculated using Eq. (48) and $y_E = 1.5$. Curve *c* displays a Coulombic potential energy, calculated utilizing Eq. (49). Values of $d=10$ Å, $\epsilon=80$, $T=293$ °K, and $Z_a Z_b = -4$ were also used to compute the curves for each case.

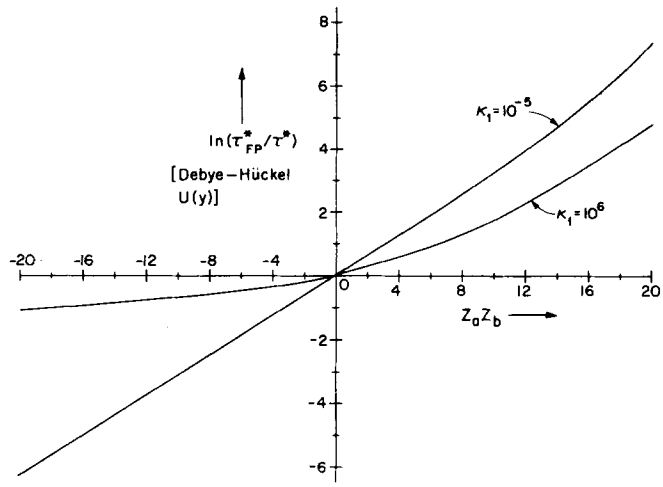

FIG. 5. $\ln(\tau^*_{FF}/\tau^*)$ vs $Z_a Z_b$ for a Debye–Hückel ionic domain–domain interaction. Results are presented for weak absorption ($\kappa_1=10^{-5}$, $\tau^*=1.77\times10^{10}$) and complete absorption ($\kappa_1=10^{6}$, $\tau^*=3.26\times10^{2}$). Additional input includes $N=100$, $L_{max}=4$, $y_N=11$, $\Delta_I=0.01$, $\tau_R^{*-1}=0$, $\kappa_0=0$, and an isotropic, uniform initial condition. Also, the protein is assumed to be in a 0.15M univalent salt solution, $d=10$ Å, $\epsilon=80$, and $T=293$ °K, so $\kappa_{DH} d = 1.272$.

Figure 4 shows the variation of these different energies with domain separation for a similar input value of $Z_a Z_b$. In all of the following calculations we have used the values $d=10$ Å, $\epsilon=80$ (i.e., H_2O as the solvent), $T=293$ °K, and an ionic strength based on a solution of 0.15M univalent salt, with the assumed protein molarity being $\ll 0.15M$. Thus, we have employed in case I the model parameter $\kappa_{DH} d \cong 1.272$ which is widely applicable in biochemical experimentation. It may be observed from Eqs. 47–49, though, that any increase in the temperature, solution ionic strength, or domain size will have an effect of decreasing $U(y)$ and will cause the mean lifetime of uncoalesced domains with forces present, τ^*_{FP}, to approach the force free value, τ^*. It can be observed from Fig. 4 that the Debye–Hückel potential, which reflects behavior in realistic liquid systems, is damped to a greater degree than the Coulombic (i.e., gas phase type) interaction.

Figures 5–7 exhibit the variation in the ration τ^*_{FP}/τ^* with differing domain–domain charges, $Z_a Z_b$. For domains that carry a small effective electronic charge (i.e., $|Z_a Z_b| \leq 4$) we can observe that $\ln(\tau^*_{FP}/\tau^*) \propto Z_a Z_b$ in cases of both weak or complete absorption. The slope

of the linear portion of each curve in the small charge region of Figs. 5–7 is particular to each case and increases as the potential energy becomes more like that of a gas phase interaction (i.e., Coulombic interaction results seen in Fig. 7 vary the greatest with charge).

The lifetimes of uncoalesced domains vary over several orders of magnitude as the domains' interactions change from the repulsive to the attractive, as revealed by our numerical results. For example, a Debye–Hückel interaction for weakly reactive domains with $Z_aZ_b = -10$ produces a lifetime $\tau^*_{FP} = 7.90\times10^8$, that is, 7.9 sec if $d = 10$ Å and $D = 10^{-6}$ cm^2/sec. A repulsive domain pair with $Z_aZ_b = 10$, on the other hand, yields $\tau^*_{FP} = 4.63\times10^{11}$ or a lifetime of 1 h 17 min. In each case we find that τ^*_{FP}/τ^* varies more for a weakly reactive system. This is indicative of the domains experiencing the diffusive effects of forces for a greater period of time as they repeatedly encounter attempting to coalesce.

As mentioned in the discussion following Eq. (18), the steady-state limit can be found in our Laplace transformed calculations utilizing $\sigma \to 0$. Thus, we can obtain the relation that links the energetics of the Smoluchowski equation to equilibrium state parameters. This assumes that the steady state of our microscopic domain pair system corresponds to the observed equilibrium state of a large number of such systems. In the examples highlighted above the steady-state limit refers to the product of a coalesced domain pair. However, for $\kappa(y,\theta) = 0$, we have calculated the concentration (or density) of uncoalesced domains in the domain's limited diffusion space for $\sigma \to 0$. We have found in actual numerical tests, as in the case of an infinite medium, that simply

$$\ln\left(\frac{C^{eq}}{C(y_i)^{eq}}\right) \cong U(y_i)\ , \tag{50}$$

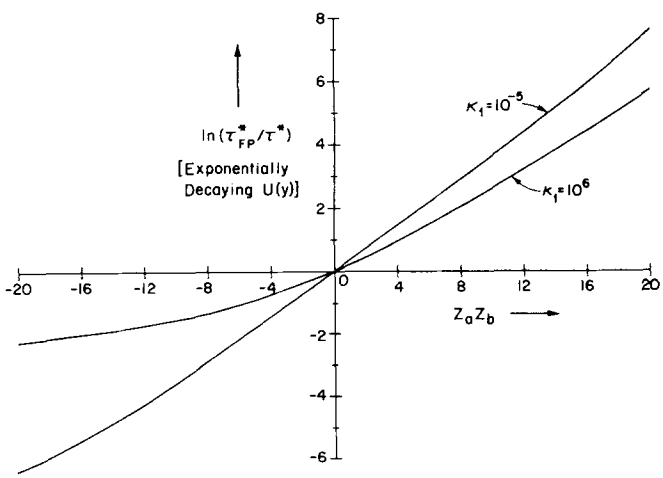

FIG. 6. $\ln(\tau^*_{FP}/\tau^*)$ vs Z_aZ_b for an exponentially decaying domain–domain interaction. Results are presented for weak absorption ($\kappa_1 = 10^{-5}$, $\tau^* = 1.77\times10^{10}$) and complete absorption ($\kappa_1 = 10^6$, $\tau^* = 3.26\times10^2$). Additional input includes $N = 100$, $L_{Max} = 4$, $y_N = 11$, $\Delta_I = 0.01$, $\tau^{*-1}_R = 0$, $\kappa_0 = 0$, $y_E = 1.5$, $d = 10$ Å, $\epsilon = 80$, $T = 293$ °K and isotropic, uniform initial condition.

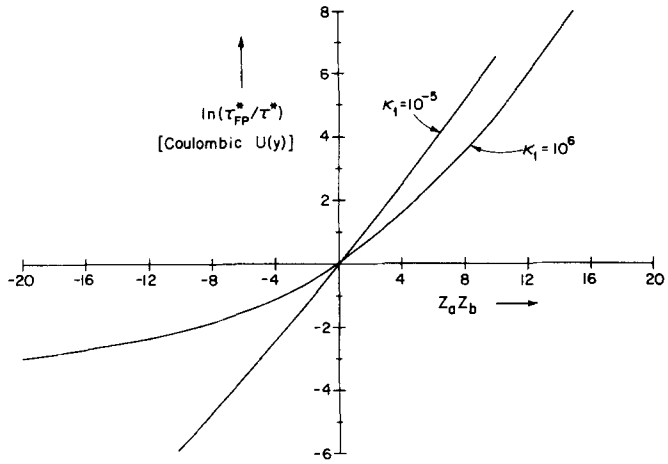

FIG. 7. $\ln(\tau^*_{FP}/\tau^*)$ vs Z_aZ_b for a simple Coulombic interaction between domains. Results are presented for weak absorption ($\kappa_1 = 10^{-5}$, $\tau^* = 1.77\times10^{10}$) and complete absorption ($\kappa_1 = 10^6$, $\tau^* = 3.26\times10^2$). Additional input includes $N = 100$, $L_{max} = 4$, $y_N = 11$, $\Delta_I = 0.01$, $\tau^{*-1}_R = 0$, $\kappa_0 = 0$, $d = 10$ Å, $\epsilon = 80$, $T = 293$ °K and an isotropic, uniform initial condition.

where C^{eq} is the "concentration" of domains in a region of diffusion space where $U(y_i) = 0$ and similarly $C(y_i)^{eq} \equiv P(i, \tau \to \infty)/[y_i V(i)]$, but where $U(y_i) \neq 0$. This is confirmation that, under conditions of no reaction or coalescence, the domains in our system will distribute themselves according to Boltzmann's rule. As in an earlier study[35] we can relate the left-hand side of Eq. (50) to a standard state chemical potential from equilibrium considerations,

$$\frac{\Delta\mu^0(y_i)}{k_BT} = \ln\left(\frac{C^{eq}}{C(y_i)^{eq}}\right)\ , \tag{51a}$$

where

$$\Delta\mu^0(y_i) \equiv \mu^0(y_i) - \mu^0 \tag{51b}$$

and μ^0 is the chemical potential in the region of space where $U(y) = 0$ and can be chosen to be zero as a reference. We then have the simple relation, using Eqs. (50) and (51),

$$\frac{\mu^0(y_i)}{k_BT} = U(y_i) \tag{52}$$

or the potential energy that we can include in our calculations is the chemical potential (or molar Gibbs free energy) that may be experimentally observed in protein studies. The results obtained in confirming Eq. (50) for the potential energies under study (cf. Fig. 4) are shown in Table IV. As in an earlier study of Zientara and Freed[35] deviations in the relationship, Eq. (50), occur when $\max|U(y)| > 1$ but it remains true as an order of magnitude indicator. For any type of potential energy where $\max|U(y)| > 1$ the simple steady-state domain distribution will deviate from that predicted from Boltzmann's relation, caused mainly by the extent and magnitude of the interaction relative to the finite size of the modeled diffusion space.

As we attempt to improve on the interactions between the domains given by Eqs. (47)–(49), we note that these

TABLE IV. $\{\ln[C^{eq}/C(y_i)^{eq}]\}/U(y_i)$ for model potentials of varying magnitude.[a]

y_i	Debye–Hückel[b]	Exponential[c]	Coulombic[d]	Hydration shell[e]
1.00	1.00	1.00	0.91	0.13
1.52	1.00	1.00	0.86	0.10
3.05	1.00	1.00	0.72	···
4.99	1.00	0.98	0.55	···
6.01	1.00	0.97	0.45	···

[a]Values for the ratio were calculated from the steady state in each case using the input $Z_a Z_b = -4$, $y_N = 11$, $\Delta = 0.01$, $N = 110$, and $\omega = 10^{-12}$. Where applicable the following additional values were used: $y_H = y_E = 1.5$, $s_H = 0.2$, $\kappa_{DH} d = 1.272$, $U_{act} = 8.714$, $U_c = -6.887$.

[b] $-1.25 \le U(y_i) \le 0$.

[c] $-1.5 \le U(y_i) \le 0$.

[d] $-2.9 \le U(y_i) \le -0.3$.

[e] $-6.8 \le U(y_i) \le 8.5$. Both the numerator and denominator of the quotient are zero for $y_i \ge 2.5$ based on the model parameters utilized.

are special cases of a more general point of view. That point of view, expressed, for example by Freed and Pedersen[29] in a related context, is to note that one should introduce the equilibrium pair-correlation function $g(r)$ for the domains in its solvent medium. Then one associates with the $g(r)$ its effective mean potential of interaction $U(r)$ by

$$\ln g(r) = -U(r)/kt \ , \tag{53}$$

so that one has from Eq. (7)

$$F(r) = \frac{\partial}{\partial r}[\ln g(r)] \ . \tag{54}$$

We wish to make use of this point of view to model in a simple fashion the hydrophobic effects of the hydration shell.[23,47–51] We conceive of this model as involving two dominant features: (1) the presence of the solvent shell reduces the $g(r)$ [raises $U(r)$] between two nonpolar side chains for values of r less than their solvent separated distance; and (2) with the solvent displaced and the two nonpolar groups in contact (i.e., $r = d$) the favored energetic state associated with the coalescence leads to an increase in $g(r)$ [i.e., a decrease in $U(r)$]. These two features are illustrated in Fig. 8 for the $U(r)$. Now, via the Smoluchowski equation [Eq. (1)].these equilibrium features affect the motional dynamics. [Of course, there can also be dynamical effects due to the solvent; these are usually modeled as an r dependent diffusion coefficient $D(r)$,[52] but we are not including this refinement here.] Now we can express Fig. 8 in simple functional form as:

Case IV. Hydration shell model interaction

$$U(y) = U_{act} \exp\{-[(y - y_H)/s_H]^2\} + U_c \exp\{-[(y-1)/\tfrac{1}{2}(y_H - 1)]^2\} \ , \tag{55}$$

where y_H is the domain separation corresponding to the maximum in the potential energy barrier due to the solvent-shell, s_H is a dimensionless length associated with the spatial extent of the hydration shell, and U_{act} and U_c are the energy parameters associated with the activation energy barrier and the coalescence energy, respectively. Figure 8 is actually obtained from Eq. (55) for the values of U_{act}, U_c, y_H, and s_H that are given, and it illustrates that although U_c is not precisely $U(d)$ [and U_{act} is not precisely $U(y_H d)$], they are similar in magnitude.

In our further considerations we wish to roughly estimate values for these parameters based on the shell model used by Scheraga and co-workers[23,47] in the conformational energy calculations on amino acid residues. Némethy and Scheraga[43] used parameters derived from the properties of hydrocarbons in solution to compute the thermodynamic paramters for the formation of hydrophobic bonds for pairs of side chains of amino acids. We have chosen the coalescence parameter U_c to be an order of magnitude larger in value, thereby estimating the energy associated with a *group* of hydrophobic residues on one domain coalescing with a *patch* of nonpolar residues on another domain. From Eq. (52) we note that U_c is directly related to the experimentally observed ΔG^0 for the coalescence process. Clearly, the proximity of polar or charged groups, as well as those residues capable of participating in hydrogen bonding will also affect ΔG^0, but have not been included in our calculations.

The entire transition from an unfolded polypeptide chain to the native structure of the protein in the presence of solvent is known to occur with a net lowering of the system Gibbs free energy on the order of 1–15 kcal/mole.[53] Therefore, we have chosen the coalescence parameter U_c, which represents the energy change of a single step in this overall process to be in this range. Similarly, we shall employ values for the activation parameter U_{act} that are consistent with experimentally determined activation energies for the conversion between denatured and native states.[26,54,55]

From the definitions of this model and the form of Eq. (55) (graphically depicted in Fig. 8), it is assumed

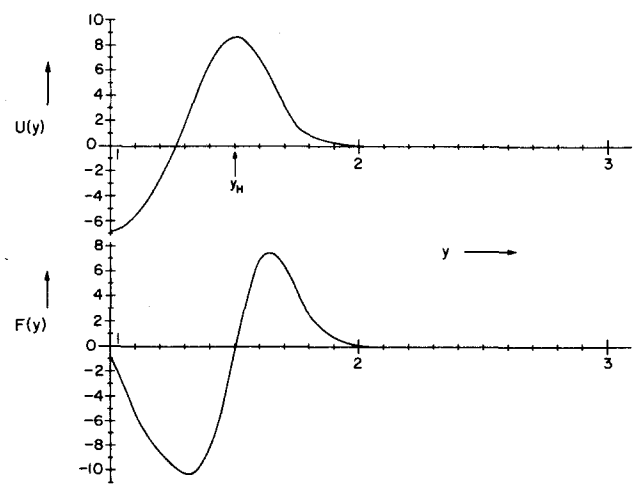

FIG. 8. Potential energy and force as functions of interdomain separation used to simulate the interaction of domains with surrounding hydration shells. This example was produced using the parametera $U_c = -6.887$ and $U_{act} = 8.714$ [i.e., $U(d) \cong -4$ kcal, $U(y_H d) = 5$ kcal] applied in Eq. (55).

that a completely absorptive reactivity would be appriate, i.e., $\kappa_{eff} \gg 1$. This implies that the penetration of the activation barrier by a domain pair is a sufficient initiator of coalescence. However, this model can also be used for weak reactivity, i.e., $\kappa_{eff} \ll 1$, which would simulate domains that traverse the hydration shell activation barrier, i.e., coalesce, but also retain the possibility of dissociating, hence producing transitory protein unfolding. Tables V and VI provide results that show that the model based on Eq. (55) reveals the above-mentioned physical characteristics. That is, for the case of complete absorption, $\kappa_1 = 10^6$, the coalescence lifetimes are independent of U_c (Table V) but almost totally dependent on the position, height, and extent of the activation barrier (Table VI), as coalescence is attained merely by the traversing of this barrier. In contrast with this is a case of weak reactivity, $\kappa_1 = 10^{-5}$, where coalescence lifetimes show a strong dependence on the coalescence energy. The allowed unfolding for $|U_c| \lesssim 10$ in this case causes a significant increase in τ^*_{FP}, which is assumed to account for permanently coalesced pairs only.

Table VI shows the ratio τ^*_{FP}/τ^* with the variations in the height of the hydration shell activation barrier and the spatial location of the barrier. As expected the existence of a barrier in close proximity to the coalescence region causes an increase in the lifetimes of the uncoalesced domain pairs. If the barrier is located farther away from the coalescence region, e.g., $y_H = 3.0$, the slowing effect of the barrier is overcome to a degree by the attraction of the domains after penetration of the shell. When the spatial extent of the hydration shell is increased (note the values for $s_H = 0.5$ in parentheses in Table VI) the slowing of the coalescence of the domains is emphasized; thus τ^*_{FP} increases and $\tau^*_{FP}/\tau^* \gtrsim 1$ in most instances studied.

The effect of an anisotropic initial condition on the results from our hydration shell model was also investigated. These results, presented in Table VII, show similar variations as the force free case seen in Table III. In all examples utilizing anisotropic initial conditions the domains were initially separated by y_I, such that $y_I > y_H > 1$. Again, the orientation dependent effects are damped out for either weak or complete absorption and are finite, yet small, in the mid range of reactivities. The case of complete absorption, which disallows domain dissociation in our model, thus is not sensitive to the initial orientation of the domains.

TABLE V. τ^*_{FP}/τ^* vs the coalescence energy parameter of the hydration shell model.[a]

U_c	$\kappa_1 = 10^{-5}$	10^6
0.0	10.01	1.24
−3.44	6.54	1.15
−6.88	4.25	1.09
−10.32	2.73	1.04
−13.76	1.73	1.00

[a]Finite difference numerical results found using the input noted above the additional parameters $U_{act} = 9.00$, $\kappa_0 = 0$, $y_N = 11$, $\Delta_I = 0.01$, $\tau_R^{*-1} = 0$, $N = 100$, $L_{max} = 4$, $y_H = 1.5$, $s_H = 0.2$, and an isotropic, delta function initial condition at $y_I = 11$. Ratios are based on the mean lifetimes of uncoalesced domains in the absence of forces given by $\tau^*(\kappa_1 = 10^{-5}) = 1.77 \times 10^9$ and $\tau^*(\kappa_1 = 10^6) = 3.84 \times 10^2$, also dependent on the input given in the preceding.

TABLE VI. τ^*_{FP}/τ^* vs barrier energy parameters of the hydration shell model.[a]

U_{act}	$y_H = 1.5$	2.0	2.5	3.0
0.0	0.87 (0.87)	0.68 (0.68)	0.51 (0.51)	0.39 (0.39)
9.0[b]	1.09 (3.19)	0.80 (2.05)	0.59 (1.39)	0.44 (0.99)
13.5	1.27 (7.80)	0.90 (4.71)	0.65 (3.07)	0.48 (2.12)
18.0	1.54 (21.61)	1.05 (12.58)	0.74 (8.01)	0.55 (5.46)

[a]Finite difference numerical results found using the input described above and $U_c = -6.88$, $\kappa_0 = 0$, $\kappa_1 = 10^6$ (complete absorption), $y_N = 11$, $\Delta_I = 0.01$, $\tau_R^{*-1} = 0$, $N = 100$, $L_{max} = 4$, and an isotropic, delta function initial condition at $y_I = 11$. Results noted first correspond to $s_H = 0.2$, with the results based on $s_H = 0.5$ following in parentheses. The mean lifetime of uncoalesced domains in the absence of forces is $\tau^* = 3.84 \times 10^2$ for the given input and initial condition.

[b]For example, $U_c = -6.88$ and $U_{act} = 9$ correspond approximately to $U(d) = -4$ kcal and $U(y_H d) = 5$ kcal at room temperature, as calculated from Eq. (55).

V. SUMMARY

We have presented a numerical method for obtaining the mean lifetimes of uncoalesced protein domain pairs including the effects of domain orientation and interdomain forces in the presence of solvent. This was accomplished by a combined treatment of the space and time dependent domain probability. First, the angular dependence of a simple domain model in which one domain has spherically symmetric properties was handled by an eigenfunction expansion method. Second, the domain separation variable was treated by the finite difference method. Finally, the coalescence yield (for a certain value of σ) was used to calculate τ^*, or τ^*_{FP} when forces are present.

Numerical results corresponded almost exactly to earlier analytic results when initial validation tests were run. The advantage of the numerical method, however, is its applicability to a wide range of physically realistic initial conditions and interactions. Also, it is not restricted to either the weak or complete absorption limits. Results were therefore presented for cases of anisotropic initial conditions, varying anisotropic reactivity, and four models of domain–domain interaction.

In all cases of reduced reactivity (i.e., $\kappa_{eff} \ll 1$) and a uniform initial condition there emerged no orientation dependent effects although an angular dependent reactivity was used. This important result emphasized that translational diffusion caused coalescence on a time scale longer than that of orientational relaxation, and this is highlighted when a low reactivity repeatedly causes long diffusive walks. The results obtained for

TABLE VII. τ^*_{FP}, mean lifetimes of uncoalesced domains in the presence of forces. Results for anisotropic initial conditions with hydration shells surrounding each domain.[a]

κ_1	$P(y,\theta,\tau=0)$ $=(4\pi)^{-1/2}(1+\cos\theta)\delta(y-y_I)$	$P(y,\theta,\tau=0)$ $=(4\pi)^{-1/2}(1-\cos\theta)\delta(y-y_I)$	Isotropic initial condition: $P(y,\theta,\tau=0)=\delta(y-y_I)$
10^{-5}	7.54×10^{9}	7.54×10^{9}	7.54×10^{9}
10	7.52×10^{3}	7.22×10^{3}	7.37×10^{3}
10^{3}	5.49×10^{2}	5.90×10^{2}	5.70×10^{2}
10^{5}	4.15×10^{2}	4.15×10^{2}	4.15×10^{2}
10^{6}	4.14×10^{2}	4.14×10^{2}	4.14×10^{2}

[a]Finite difference results found using the input values $N=100$, $L_{max}=4$, $y_N=11$, $\Delta_I=0.01$, $\tau_R^{*-1}=0$, $\kappa_0=0$, $y_I=11$, and the hydration layer simulation parameters $y_H=1.5$, $s_H=0.2$, $U_{act}=8.714$, $U_c=-6.887$.

τ^* or τ^*_{FP} using an anisotropic initial condition, on the contrary, showed a slight orientation dependence in the coalescence lifetime but only in the mid range of reactivities. Values of τ^*_{FP} for a range of domain charges showed several orders of magnitude difference from τ^*. This highlights the importance of including domain charge effects in further studies.

In simulations of the steady state in our bounded domain pair system we developed a relationship between the potential energy that enters through the Smoluchowski equation and the standard state Gibbs free energy that might emerge from biochemical experimentation. Our method, then, can be applied in direct simulations of realistic protein folding situations, a feature lacking in earlier analytic treatments.

Also, we have taken advantage of the flexibility of our approach to simulate by a simple model the effects of a hydration shell on domain diffusion. This model includes solvent shells surrounding each domain that affect domain diffusion in such a way as to cause a general slowing of the coalescence process if the shell is tightly encircling the domain or if the shell has a substantial width. Anisotropic initial conditions used with this model produced only minor orientation dependent effects, a result explained by orientational relaxation and reactivity arguments.

We have applied the arguments of diffusion-controlled kinetics to the consideration of domain coalescence in order to ultimately consider the time evolution of protein folding. The time scale for many types of structural changes in proteins has been summarized,[5] and changes in the topography of the polypeptide chain are reported to occur in the range 10^{-4}–10^{2} sec. Temperature jump and stopped flow kinetic studies have demonstrated relaxation in this time range.[2] The results presented in this work for the mean coalescence time span the reported experimental values for the various cases treated

With the appropriate choice of parameters, computational methods presented here may be used to simulate the association of domains in response to long range interactions whether they be hydrophobic in nature or due to the effects of charge, relative orientation, or hydration. Due to the generality of our approach, it is possible to include the net effect of both a hydration shell and charged domains (i.e., Debye–Hückel domain–domain interactions) by a further coupling of the energies utilized in the models of our present study.

An assumption of Brownian diffusive motion governing coalescence has been used in this model. Directing forces, which might be provided by the connecting residues in a polypeptide chain, could be incorporated in future refinements by using θ-dependent potentials or non-Brownian motion.

The numerical methods used in the preceding are also being used in a modified form in computational biochemical studies of protein unfolding and quaternary structure formation.

ACKNOWLEDGMENTS

The authors wish to thank Dr. G. Nemethy for his helpful criticism of our manuscript. J.A.N. wishes to acknowledge the guidance and support provided by Professor H. A. Scheraga.

[1]M, Karplus and D. L. Weaver, Nature **260**, 404 (1976); Biopolymers **18**, 1421 (1979).

[2]See, for example, C. B. Anfinsen and H. A. Scheraga, Adv. Protein Chem. **29**, 205 (1975); R. L. Baldwin, Ann. Rev. Biochem. **44**, 453 (1975); G. Nemethy and H. A. Scheraga, Q. Rev. Biophys. **10**, 239 (1977); T. E. Creighton, Prog. Biophys. Mol. Biol. **33**, 231 (1978); H. A. Scheraga, in *Protein Folding*, edited by R. Jaenicke (Elsevier/North Holland Biomedical Press, Amsterdam, 1980), p. 261.

[3]C. B. Anfinsen, Science **181**, 223 (1973); D. B. Wetlaufer, and S. Ristow, Annu. Rev. Biochem. **42**, 135 (1973); H. A. Scheraga, Pure Appl. Chem. **36**, 1 (1973); O. B. Ptitsyn, and A. A. Rashin, Biophys. Chem. **3**, 1 (1975); G. Nemethy, and H. A. Scheraga, Proc. Natl. Acad. Sci. USA **76**, 6050 (1979); S. Tanaka and H. A. Scheraga, Macromolecules **10**, 291 (1977); B. Honig, A. Ray, and C. Levinthal, Proc. Natl. Acad. Sci. USA **73**, 1974 (1976).

[4]C. Levinthal, J. Chem. Phys. **65**, 44 (1968); D. B. Wetlaufer, Proc. Natl. Acad. Sci. USA **70**, 697 (1973).

[5]G. Careri, P. Fasella, and E. Gratton, CRC Crit. Rev. Biochem. **3**, 141 (1975).

[6]D. H. Sachs, A. N. Schechter, A. Eastlake, and C. B. Anfinsen, Proc. Natl. Acad. Sci. USA **69**, 3790 (1972); R. R. Matheson, Jr. and H. A. Scheraga, Biochemistry **18**, 2437

(1979); L. G. Chavez, Jr. and H. A. Scheraga, *ibid.* **16**, 1849 (1977); T. C. Creighton, J. Mol. Biol. **87**, 579 (1974); J. Hochman, M. Gavish, D. Inbar, and D. Givol, Biochemistry **15**, 2706 (1976); J. M. Teale and D. C. Benjamin, J. Biol. Chem. **252**, 4521 (1977).

[7]A. Liljas and M. G. Rossmann, Ann. Rev. Biochem. 43, 475 (1974); B. W. Matthews, J. N. Jansonius, P. M. Colman, B. P. Schoenborn and D. Dupourgue, Nature (London) New Biol. **238**, 37 (1972); E. S. Rowe and C. Tanford, Biochemistry **12**, 4822 (1973).

[8]J. A. McCammon, B. R. Gelin, and M. Karplus, Nature 267, 585 (1977).

[9]J. A. McCammon, P. G. Wolynes, and M. Karplus, Biochemistry **18**, 927 (1979).

[10]S. Tanaka and H. A. Scheraga, Proc. Natl. Acad. Sci. USA **72**, 3802 (1975); P. J. Rossky, M. Karplus, and A. Rahman, Biopolymers **18**, 825 (1979); A. T. Halger and J. Moult, Nature (London) **272**, 222 (1978).

[11]G. Wilemski and M. Fixman, J. Chem. Phys. **60**, 866 (1974); *ibid.* **60**, 878 (1974); G. T. Evans, Mol. Phys. **38**, 1201 (1979).

[12]R. Noyes, Prog. React. Kinet. **1**, 129 (1961).

[13]See, for example, J. Freire and M. Fixman, J. Chem. Phys. **69**, 634 (1978); D. C. Rapaport, J. Chem. Phys. **71**, 3299 (1979).

[14]See, for example, M. Fixman, J. Chem. Phys. **69**, 1527 (1978); **69**, 1538 (1978); D. L. Ermak and J. A. McCammon, *ibid.* **69**, 1352 (1978); J. A. Montgomery, Jr., D. Chandler, and B. Berne, *ibid.* **70**, 4056 (1979); *Report on the Workshop-Stochastic Molecular Dynamics*, edited by D. Ceperley (Natl. Res. for Comp. in Chemistry, Berkeley, California, 1979).

[15]G. P. Zientara and J. H. Freed, J. Phys. Chem. **83**, 3333 (1979).

[16]M. Von Smoluchowski, Ann. Phys. (Leipzig) **48**, 1103 (1915); Z. Phys. Chem. **92**, 129 (1917).

[17]K. Solc and W. H. Stockmayer, J. Chem. Phys. **54**, 2981 (1971); Int. J. Chem. Kinet. **5**, 733 (1973).

[18]K. S. Schmitz and J. M. Schurr, J. Phys. Chem. **76**, 534 (1972).

[19]K. Salikov, Theor. Eksp. Khim. **13**, 731 (1977).

[20]M. Doi, Chem. Phys. **11**, 107 (1975); *ibid.* **11**, 115 (1975).

[21]T. L. Hill, Proc. Natl. Acad. Sci. USA **72**, 4918 (1975).

[22]C. Tanford, J. Am. Chem. Soc. **84**, 4240 (1962); I. Z. Steinberg, and H. A. Scheraga, J. Biol. Chem. **238**, 172 (1963); Z. I. Hodes, G. Némethy, and H. A. Scheraga, Biopolymers, **18**, 1565 (1979).

[23]H. A. Scheraga, Acc. Chem. Res. **12**, 7 (1979).

[24]M. Levitt and C. Chothia, Nature **261**, 552 (1976); F. E. Cohen, T. J. Richmond, and F. M. Richards, J. Mol. Biol. **132**, 275 (1979).

[25]J. S. Richardson, Proc. Natl. Acad. Sci. USA **73**, 2619 (1976); Nature **268**, 495 (1977); M. J. E. Sternberg and J. M. Thornton, J. Mol. Biol. **105**, 367 (1976); **110**, 269, 285 (1977); **115**, 1 (1977).

[26]R. R. Matheson, Jr. and H. A. Scheraga, Macromolecules **11**, 819 (1978); M. I. Kanehisa and T. Y. Tsong, Biopolymers **18**, 2913 (1979).

[27]S. J. Wodak and J. Janin, Proc. Natl. Acad. Sci. USA **77**, 1736 (1980).

[28]G. Adam and M. Delbrück, in *Structural Chemistry and Molecular Biology*, edited by A. Rich and W. Davidson (Freeman, San Francisco, 1968).

[29]J. H. Freed and J. B. Pedersen, Adv. Magn. Reson. **8**, 1 (1976).

[30]F. C. Collins and G. E. Kimball, J. Colloid Sci. **4**, 425 (1949).

[31]J. B. Pedersen, *Chemically Induced Magnetic Polarization: Theory, Technique, and Applications*, edited by L. Muus, P. W. Atkins, K. A. McLauchlan, and J. B. Pedersen (Reidel, The Netherlands, 1977), Chap. XVII.

[32]The boundary condition of Collins and Kimball (Ref. 30) does not include any orientation dependent qualities. However, Solc and Stockmayer (Ref. 17) have extended the concept of a partially absorbing inner boundary to include the orientation of the particles upon contact.

[33]This constraint can be included when utilizing the Stokes–Einstein formulas, which rigorously pertain to only freely diffusing spherical particles, by the restriction of $R=0$ irrespective of the magnitude of r_b. The value of D is not affected by this constraint.

[34]G. P. Zientara and J. H. Freed, J. Chem. Phys. **70**, 1359 (1979); **70**, 2587 (1979).

[35]G. P. Zientara and J. H. Freed, J. Chem. Phys. **72**, 1285 (1980).

[36]J. H. Freed, G. V. Bruno, and C. F. Polnaszek, J. Phys. Chem. **75**, 3385 (1971); A. E. Stillman, G. P. Zientara, and J. H. Freed, J. Chem. Phys. **71**, 113 (1979).

[37]S. Chandrasekhar, Rev. Mod. Phys. **15**, 1 (1943).

[38]G. P. Zientara and J. H. Freed, J. Chem. Phys. **71**, 3861 (1979).

[39]For example, if $d=10$ Å and $D=10^{-6}$ cm^2/sec then $\tau^*=10^{10}$ corresponds to a lifetime of 100 sec and $\tau^*=10^7$ corresponds to 0.1 sec.

[40]D. L. Weaver, Biophys. Chem. **10**, 245 (1979).

[41]R. H. Haschemeyer and A. E. V. Haschmeyer, in *Proteins: A Guide to Study by Physical and Chemical Methods* (Wiley, New York, 1973), pp. 109–129.

[42]J. B. Pedersen and J. H. Freed, J. Chem. Phys. **59**, 2869 (1973); S. A. Rice, P. R. Butler, M. J. Pilling, and J. K. Baird, *ibid.* **70**, 4001 (1979).

[43]G. Némethy and H. A. Scheraga, J. Phys. Chem. **66**, 1773 (1962).

[44]P. Debye, Trans. Electrochem. Soc. **82**, 265 (1942); P. Debye, and E. Hückel, Phys. Z. **24**, 185 (1923); **24**, 305 (1923).

[45]J. Deisenhofer and W. Steigemann, Acta Crystallogr. Sect. B **31**, 238 (1975).

[46]F. A. Quiocho and W. N. Lipscomb, Adv. Protein Chem. **25**, 1 (1971).

[47]W. Kauzmann, Adv. Protein Chem. **14**, 1 (1959).

[48]F. Franks and D. Eagland, CRC Crit. Rev. Biochem. 3, 165 (1975).

[49]I. D. Kuntz, Jr. and W. Kauzmann, Adv. Protein Chem. **28**, 239 (1974).

[50]Z. I. Hodes, G. Némethy, and H. A. Scheraga, Biopolymers **18**, 1611 (1979); K. D. Gibson and H. A. Scheraga, Proc. Natl. Acad. Sci. USA **58**, 420 (1967).

[51]A. J. Hopfinger, Macromolecules **4**, 731 (1971).

[52]S. H. Northrup and J. T. Hynes, J. Chem. Phys. **71**, 871 (1979).

[53]P. L. Privalov and N. N. Khechinashvili, J. Mol. Biol. **86**, 665 (1974); C. N. Pace, Crit. Rev. Biochem. **3**, 1 (1975); R. Lumry and R. Biltonen, in *Structure and Stability of Biological Macromolecules*, edited by S. N. Timasheff and G. D. Fasman (Marcel Dekker, New York, 1969), pp. 65–212.

[54]H. F. Epstein, A. N. Schechter, R. F. Chen, and C. B. Anfinsen, J. Mol. Biol. **60**, 499 (1971).

[55]J. F. Brandts, H. R. Halvorson, and M. Brennan, Biochemistry **14**, 4953 (1975).